

**Project Report  
ATC-247**

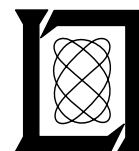
**ASR-9 Weather System Processor (WSP):  
Wind Shear Algorithms Performance Assessment**

**M.E. Weber  
J.A. Cullen  
S.W. Troxel  
C.A. Meuse**

**7 May 1996**

---

**Lincoln Laboratory**  
MASSACHUSETTS INSTITUTE OF TECHNOLOGY  
*LEXINGTON, MASSACHUSETTS*



---

Prepared for the Federal Aviation Administration,  
Washington, D.C. 20591

This document is available to the public through  
the National Technical Information Service,  
Springfield, VA 22161

This document is disseminated under the sponsorship of the Department of Transportation in the interest of information exchange. The United States Government assumes no liability for its contents or use thereof.

1. Report No. ATC-247		2. Government Accession No.		3. Recipient's Catalog No.	
4. Title and Subtitle  ASR-9 Weather System Processor (WSP): Wind Shear Algorithms Performance Assessment				5. Report Date 7 May 1996	
				6. Performing Organization Code	
7. Author(s) Mark E. Weber, Joseph A. Cullen, Seth W. Troxel, and Cynthia A. Meuse				8. Performing Organization Report No. ATC-247	
9. Performing Organization Name and Address  Lincoln Laboratory, MIT 244 Wood Street Lexington, MA 02173-9108				10. Work Unit No. (TRAIS)	
				11. Contract or Grant No. DTFA01-93-Z-02012	
12. Sponsoring Agency Name and Address Department of Transportation Federal Aviation Administration Washington, DC 20591				13. Type of Report and Period Covered Project Report	
				14. Sponsoring Agency Code	
15. Supplementary Notes  This report is based on studies performed at Lincoln Laboratory, a center for research operated by Massachusetts Institute of Technology under Air Force Contract F19628-95-C-0002.					
16. Abstract  <p style="text-align: center;">Lincoln Laboratory has developed a prototype Airport Surveillance Radar Weather Systems Processor (ASR-WSP) that has been used for field measurements and operational demonstrations since 1987. Measurements acquired with this prototype provide an extensive data base for development and validation of the algorithms the WSP uses to generate operational wind shear information for Air Traffic Controllers. This report assesses the performance of the current versions of the WSP's microburst and gust front wind shear detection algorithms on available data from each of the WSP's operational sites. Evaluation of the associated environmental characteristics (e.g., storm structure, radar ground clutter environment) allows for generalization of results to the other major U.S. climatic regimes where the production version of WSP will be deployed.</p>					
17. Key Words  low-altitude wind shear weather systems processor microburst gust front			18. Distribution Statement  This document is available to the public through the National Technical Information Service, Springfield, VA 22161.		
19. Security Classif. (of this report)  Unclassified		20. Security Classif. (of this page)  Unclassified		21. No. of Pages  42	22. Price

## **ABSTRACT**

Lincoln Laboratory has developed a prototype Airport Surveillance Radar Weather Systems Processor (ASR-WSP) that has been used for field measurements and operational demonstrations since 1987. Measurements acquired with this prototype provide an extensive database for development and validation of the algorithms the WSP uses to generate operational wind shear information for Air Traffic Controllers. This report assesses the performance of the current versions of the WSP's microburst and gust front wind shear detection algorithms on available data from each of the WSP's operational sites. Evaluation of the associated environmental characteristics (e.g., storm structure, radar ground clutter environment) allows for generalization of results to the other major U.S. climatic regimes where the production version of WSP will be deployed.

## TABLE OF CONTENTS

<b><u>Section</u></b>	<b><u>Page</u></b>
Abstract	iii
List of Illustrations	vii
List of Tables	vii
1.0 INTRODUCTION	1
2.0 WSP PROTOTYPE SYSTEM, DATA PROCESSING ALGORITHMS AND PERFORMANCE ASSESSMENT METHODOLOGY	5
2.1 Prototype System Overview	5
2.2 Synopsis of Relevant Algorithms	8
A. Base Data Generation Algorithms	8
B. Microburst Detection Algorithm	8
C. Gust Front Detection Algorithm	8
2.3 Scoring Methodology	9
A. Microburst Algorithm	9
B. Gust Front Algorithm	9
3.0 WIND SHEAR DETECTION PERFORMANCE AT PROTOTYPE OPERATING SITES	11
3.1 Huntsville, Alabama, 1987-1988	11
A. Testbed Configuration	11
B. Truth Sensors	11
C. Environmental Characteristics	11
D. Microburst Detection Performance	13
3.2 Kansas City, Kansas, 1989	14
A. Testbed Configuration	14
B. Truth Sensors	14
C. Environmental Characteristics	14
D. Microburst Detection Performance	16
3.3 Orlando Florida, 1990-1992	17
A. Testbed Configuration	17
B. Truth Sensors	17
C. Environmental Characteristics	17
D. Microburst Detection Performance	19
E. Gust Front Detection Performance	19

**TABLE OF CONTENTS**  
**(Continued)**

<b><u>Section</u></b>	<b><u>Page</u></b>
3.4 Albuquerque, New Mexico 1993-1995	20
A. Testbed Configuration	20
B. Truth Sensors	20
C. Environmental Characteristics	20
D. Microburst Detection Performance	22
E. Gust Front Detection Performance	23
4.0 INTERPRETATION OF RESULTS RELATIVE TO WSP NATIONAL DEPLOYMENT PLANS	25
5.0 PERFORMANCE OF CURRENT GROUND-BASED WIND SHEAR DETECTION SYSTEMS	27
6.0 SUMMARY	29
APPENDIX A: CLIMATOLOGICAL DATA FOR PROPOSED WSP SITES	31
REFERENCES	33

## LIST OF ILLUSTRATIONS

<b><u>Figure</u></b>	<b><u>Page</u></b>
1. Geographic Situation Display (GSD) (left) and ribbon display terminal (RDT) (right) that convey information on wind shear and other weather phenomena to controllers.	2
2. A high-level block diagram of the prototype Weather Systems Processor.	6
3. The host ASR-9 and prototype WSP at their current locations on Albuquerque International Airport.	7
4. Map showing locations of FAA/Lincoln Laboratory ASR-8 testbed, supporting C-band pencil-beam “truth radar” and Mesonet anemometer during 1987-1988 Huntsville campaign.	12
5. Map showing locations of FAA/Lincoln Laboratory WSP and TDWR testbeds at Kansas City and supporting University of North Dakota radar.	15
6. Map showing locations of sensor deployed in Orlando, Florida during TDWR and WSP field measurement programs there.	18
7. Map showing locations of WSP testbed, MIT “truth” radar, and anemometers at Albuquerque.	21

## LIST OF TABLES

<b><u>Table</u></b>	<b><u>Page</u></b>
1. ASR-9 Microburst Detection Algorithm Scoring Results for Huntsville	13
2. ASR-9 Microburst Detection Algorithm Scoring Results for Kansas City	16
3. ASR-9 Microburst Detection Algorithm Scoring Results for Orlando	19
4. ASR-9 Gust Front Detection Algorithm Scoring Results for Orlando	19
5. ASR-9 Microburst Detection Algorithm Scoring Results for Albuquerque	23
6. ASR-9 Gust Front Detection Algorithm Scoring Results for Albuquerque	23
7. Projected WSP Microburst Detection Performance Within Climatological Regimes ( $\Delta V \geq 15$ m/s )	26
8. Performance Summaries for Current Ground Based Wind Shear Detection Equipment	28



Figure 1. Geographic Situation Display (GSD) (left) and ribbon display terminal (RDT) (right) that convey information on wind shear and other weather phenomena to controllers.



## 1.0 INTRODUCTION

Under Federal Aviation Administration sponsorship, Lincoln Laboratory has developed a prototype Airport Surveillance Radar Weather Systems Processor (ASR-WSP). This prototype has been used for field measurements and operational demonstrations since 1987. Measurements so acquired provide an extensive database for development and validation of the algorithms used by the WSP to generate operational wind shear information for Air Traffic Controllers. In this report we assess the performance of the current versions of the WSP's microburst and gust front wind shear detection algorithms on available data from each of the locations at which our prototype system has operated. Evaluation of the associated environmental characteristics (e.g., storm structure, radar ground clutter environment) allows for generalization of these results to the major U.S. climatic regimes where the production version of WSP will be deployed.

The WSP addresses two forms of thunderstorm-generated low-altitude wind shear. Microbursts occur when intense, small-scale downdrafts from thunderstorms reach the earth's surface and diverge horizontally in a roughly cylindrically symmetric pattern. Aircraft penetrating the resulting surface wind outflow encounter a dangerous headwind to tailwind velocity transition (i.e., loss of airspeed) and may experience additional control problems associated with the core downdraft or other smaller scale circulations in the microburst. Microburst onset times may be extremely short, with the divergent outflow reaching peak intensity within a few minutes of the downdraft first reaching the surface.

Gust fronts are the leading boundary of larger-scale thunderstorm outflows which may propagate tens of kilometers away from the generating precipitation. Convergent wind shear (i.e., an increasing headwind) encountered by an aircraft penetrating a gust front is considered less hazardous than the loss associated with a microburst. The winds behind the front, however, are turbulent and the long-term change of wind speed/direction following passage of the front affects runway operations. Tracking and predicting gust front arrivals before they reach an airport allows for more efficient use of runways.

Figure 1 shows the dedicated displays by which the WSP conveys information on wind shear and other weather phenomena to controllers. Runway-specific microburst alerts (losses equal to or exceeding 30 kts or approximately 15 m/s ) or wind shear alerts (losses less than 30 kts and all gains) are displayed on an alphanumeric ribbon display terminal (RDT) to be read verbatim to affected pilots by the Tower local controller. A color Geographic Situation Display (GSD) provides ATC supervisory personnel general information on convective weather in terminal airspace, showing the location and movement of thunderstorm cells and gust fronts and the position of microbursts. This information is generated in a totally automated fashion using computer algorithms that:

1. Process the "raw" echoes received by the radar to generate base data, which is imagery of precipitation reflectivity and Doppler spectrum content; and
2. Recognize operationally relevant features in the spatio-temporal structure of these base data images; for example, the presence, intensity and movement of low-altitude wind shear.

The accuracy of the operational products provided by the WSP is a function of both stages of algorithm processing. The performance assessments provided here are end-to-end in the sense that “truth” for the wind shear products scoring is provided by examination of data from sensors (generally pencil-beam weather radar) that are independent of the ASR-9.

The organization of this report is as follows. Section 2 provides background on the WSP prototype system, its data processing algorithms, and the scoring methodology we have used to quantify performance. For each of the testbed deployment sites, Section 3 describes relevant radar configuration details, information on the weather and ground clutter environment, and finally, the results of our microburst and gust front detection performance assessment. In Section 4 we summarize expected wind shear characteristics in the major U.S. climatic regimes in which the WSP will be deployed and use the results of our site-specific analysis to estimate WSP performance in each regime. For comparison with these WSP performance metrics, we summarize data on the wind shear detection performance of current FAA ground-based wind shear detection equipment in Section 5.

## **2.0 WSP PROTOTYPE SYSTEM, DATA PROCESSING ALGORITHMS AND PERFORMANCE ASSESSMENT METHODOLOGY**

The FAA/Lincoln Laboratory WSP testbed was originally deployed in 1987, hosted on an ASR-8, and instrumented primarily to acquire and record quadrature video samples for both high- and low-beam receive paths out to the range of operational concern for wind shear detection. A real-time signal processor was added in 1988, and full-up WSP prototype operational tests began in 1990 and have continued each summer thereafter. Throughout these later operations, full capability to archive both base data and "raw" radar samples has been maintained. In this section, we describe relevant details of the testbed configuration, the data processing algorithms that have been developed to generate wind shear products, and the methodology we employ to quantify performance.

### **2.1 Prototype System Overview**

Figure 2 is a high-level block diagram of the prototype Weather Systems Processor as it has operated since our first operational demonstration in 1990. The system is comprised of:

1. An ASR-8 or ASR-9 host radar;
2. Interfaces to extract necessary radio frequency (RF) and timing signals;
3. Identical receivers and A/D converters for the high- and low-beam receiving channels of the host radar;
4. A digital signal processor that suppresses interference (e.g., ground clutter) and computes base data (i.e., estimates of weather reflectivity, Doppler velocity and spectrum width for each range-azimuth resolution cell);
5. Recorders to archive both unprocessed in-phase and quadrature (I and Q) radar samples, and base data;
6. Single-board computers and workstations that run the microburst and gust front detection algorithms, the storm motion algorithm, generate precipitation reflectivity maps, and transmit the resulting products to the air traffic control tower; and
7. Remote workstations and monitors that provide graphical and alphanumeric displays to air traffic controllers and their supervisors.

Prior to 1990, the prototype did not include the processors used to generate real-time meteorological product information (microburst, gust front, storm motion, precipitation) and the GSD server. The VME-bus signal processor and local displays were not present until 1989.

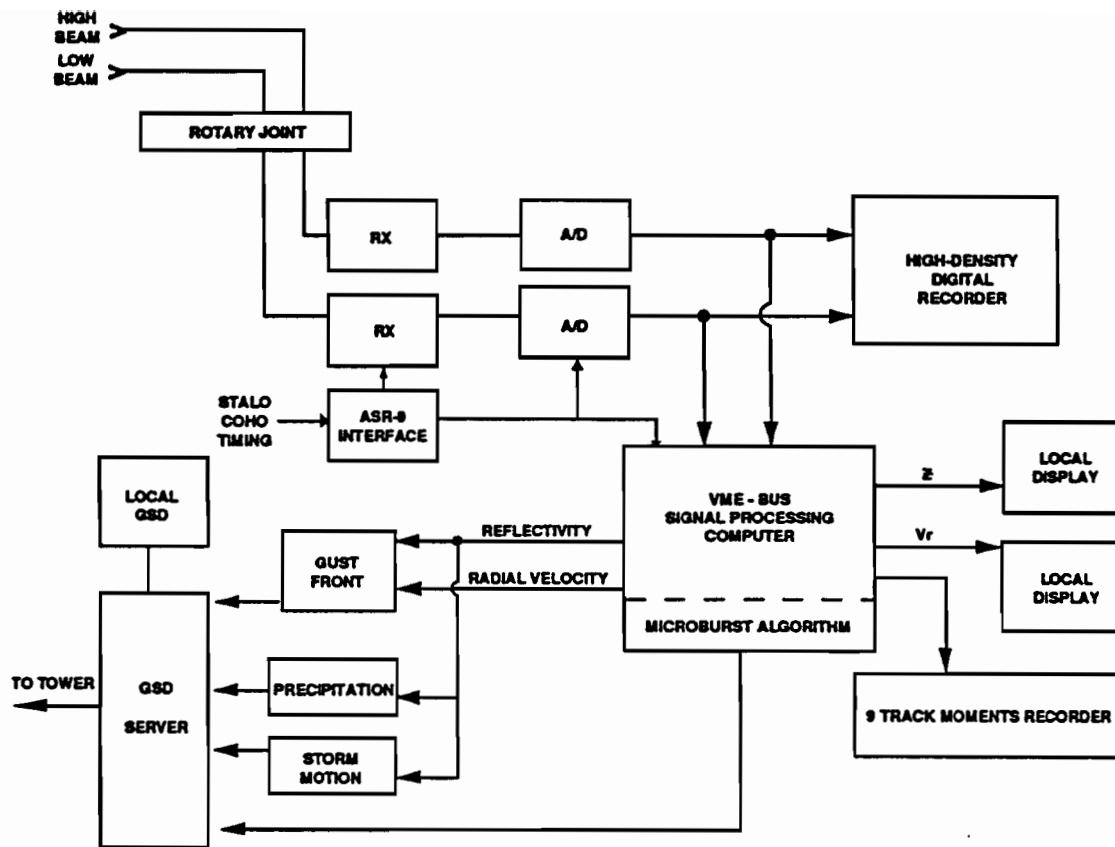
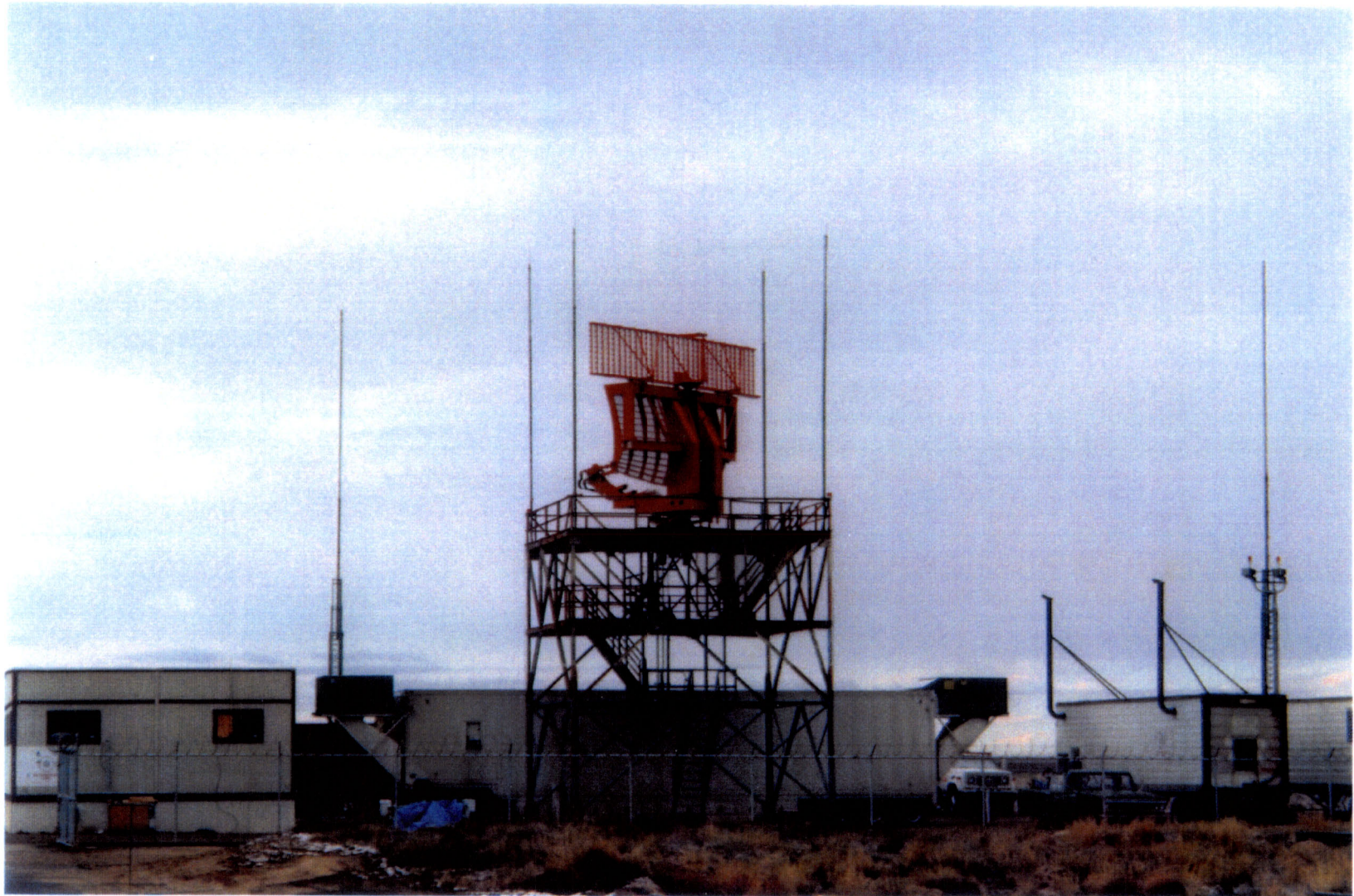


Figure 2. A high-level block diagram of the prototype Weather System Processor.

Figure 3 is photograph of the host ASR-9 and prototype WSP at their current locations on Albuquerque International Airport. Both channels of the ASR-9 (transmit and receive cabinets, target processors, six-level weather processors, and Remote Monitoring System) are deployed in a mobile fifty-foot trailer. This trailer also houses the signal interface module, receivers, and A/D converters for the WSP. Digitized signals are transmitted over a fiber optic link to the adjacent office trailer which contains the data processing and recording systems.

It is important to note that this prototype has not fully emulated engineering design details that will be realized with the production WSP. In particular, the prototype's receive chain design has evolved over the testbed's operating history in order to achieve increasing sensitivity for the detection of "dry" wind shear phenomena such as gust fronts. During its early years of operation, net receive chain sensitivity was 5 to 15 dB less than will be achieved with the production WSP. This fact precludes quantitative assessment of gust front detection capability at the first two prototype sites (Huntsville and Kansas City).



*Figure 3. The host ASR-9 and prototype WSP at their current locations on Albuquerque International Airport.*



## 2.2 Synopsis of Relevant Algorithms

### A. Base Data Generation Algorithms

The principal elements of the base data generation algorithms are described in Weber [1987, 1989]. For each radar resolution cell, these algorithms suppress ground clutter and estimate the reflectivity, mean low-altitude Doppler velocity and spectrum width of the meteorological echoes. High- and low-beam signals are processed on alternating scans of the antenna. Ground clutter suppression is accomplished using a data adaptive approach that minimizes distortion of the weather echo spectrum in the filtering process. The output of the clutter suppression module is passed to an auto-correlator that generates estimates of the signal auto-correlation function for both high and low beams at delays from zero to four times the average pulse repetition interval.

The precipitation reflectivity factor, Doppler velocity and spectrum width are calculated using the output of the auto-correlator. Data quality flags are generated where contamination from ground clutter breakthrough, out-of-trip weather and velocity folding occur and are used by the meteorological product algorithms in assessing the validity of associated base data.

### B. Microburst Detection Algorithm

The WSP microburst detection algorithm is a two-stage process. The first stage, described by Newell and Cullen [1993], searches for candidate divergence signatures in the low-altitude Doppler velocity field. A straightforward radial-by-radial search is performed for the characteristic increasing (with range) velocity signature associated with microburst outflows. The resulting shear segments are then subjected to scan-to-scan continuity tests, grouped azimuthally and passed on to the second stage verification process that ensures that the candidate microburst detections are physically plausible. This verification process utilizes advanced image processing and expert system technology to assess whether the spatial and temporal structure of the liquid water (i.e., reflectivity) field associated with candidate microburst detections is consistent with physical expectations.

### C. Gust Front Detection Algorithm

The WSP's Machine Intelligent Gust Front Detection algorithm [Delanoy and Troxel, 1993] exploits image processing/expert system technology developed at Lincoln Laboratory originally in the context of Automatic Target Recognition. MIGFA employs multiple, independent functional template correlators that search the WSP's reflectivity and Doppler velocity imagery for features that are selectively indicative of gust fronts. Because the ASR-9's intrinsic sensitivity is often inadequate to directly measure the convergent radial velocity pattern associated with gust fronts, MIGFA's feature detectors are designed to recognize manifestations of the *thin line echo* along a front's leading edge. This subtle feature can be recognized as a slight enhancement in radar reflectivity relative to background and/or as a line of spatially coherent Doppler velocity estimates embedded in a noise background where gate-to-gate estimate variance is much higher. Movement of thin lines through a background of stationary ground clutter residue and slower moving storm cells aids in their identification.

The outputs of the feature detectors are expressed as interest images, whose values (0 to 1) specify the degree of evidence that a gust front is present. The multiple interest images are fused to form an overall map of evidence indicating the locations of possible gust fronts. From this

image, fronts are extracted as chains of points (events) and correlated with prior events to establish speed and direction of motion. Forecasts of gust front/wind shift impact at an airport are generated by extrapolating the front's current position using this motion estimate.

## **2.3 Scoring Methodology**

### **A. Microburst Algorithm**

The performance scoring utilized in this report characterizes the end-to-end capability of the WSP microburst detection system (i.e., sensor, base data generation algorithms and meteorological product generation algorithms) to automatically detect loss-inducing wind shear. Truth is generated through manual examination of the base data fields generated by the supporting sensors (principally pencil-beam weather radars such as the Lincoln/FAA TDWR testbed) described in Section 3. User-interactive software allows the analyst to draw, with a mouse, arbitrarily shaped polygons over the displayed data to enclose microbursts or wind shears with loss. Coordinates defining these polygons are entered into the truth database for automatic comparison with the corresponding shapes that define detections from the WSP. Note that the supporting radars often scanned only a portion of the area covered by the WSP and typically updated their near-surface data at intervals of one to three minutes. WSP detections that were outside the areas covered by the truth radars or were displaced by more than 30 seconds from the nearest truth radar scan were not scored.

A hit is defined as a WSP-generated microburst shape that overlaps a truth polygon. Should more than one WSP-generated shape overlap a truth, only one hit is tabulated. A false alarm is tabulated for each WSP-generated report that does not intersect a truth polygon.

Probability of detection ( $P_d$ ) is defined as the ratio of the number of hits to the total number of wind shear polygons in the truth database. Probability of false alarm ( $P_{fa}$ ) is the ratio of the number of false alarms to the total number of WSP reports (i.e., the sum of hits and false alarms). In this report, both statistics are presented for categories of increasing microburst intensity. The categories for  $P_d$  refer to the differential velocities of the events considered in the truth database. Thus, for the “ $\geq 15$  m/s” category, wind shear events with true differential velocity of less than 15 m/s are effectively deleted from the truth database in calculating  $P_d$ . For  $P_{fa}$ , these categories refer to the differential velocity reported by the WSP algorithms. Thus, again considering the “ $\geq 15$  m/s” category, WSP reports with differential velocity less than 15 m/s would not be considered in tabulating false alarms.

### **B. Gust Front Algorithm**

Gust front hit-miss statistics are tabulated analogously to those presented for the microburst algorithm. Truth polygons in this case are taken as elongated eight-kilometer-wide corridors centered on the line of maximum velocity convergence and/or thin line intensity as determined from the truth radar data. Hits, false alarms,  $P_d$  and  $P_{fa}$  are then calculated as above based on whether the WSP's reported gust front lines intersect or miss truth polygons. The relatively broad width of the truth polygon accounts for the finite extent of the region of convergent shear associated with a gust front and for time differences between available near-surface data from the truth radar and the WSP reports. A maximum time difference of two minutes is allowed before the WSP reports are not scored.

### 3.0 WIND SHEAR DETECTION PERFORMANCE AT PROTOTYPE OPERATING SITES

#### 3.1 Huntsville, Alabama, 1987-1988

##### A. Testbed Configuration

One channel of a Navy ASR-8 was deployed to a site just west of the airport in Huntsville, Alabama in the summer of 1986. The radar and associated quadrature video recording system were operational by autumn, and the first Doppler weather imagery from the testbed was generated (off line from the recorded raw radar data) over the winter. Based on the successful summer 1987 off-line demonstration that microburst and gust front signatures could be extracted from the testbed signals, a first implementation of a real-time signal processor was deployed in 1988. This facilitated effective data collection, monitoring, and scoring.

The net effect of the ASR-8 parameters and the WSP receive chain configuration was to substantially reduce receiver sensitivity relative to that of the current prototype and the production WSP. Net reduction in low-beam sensitivity was 16 dB at 5 km and 6.5 dB at 15 km. In Huntsville, this would not likely have affected results for the microburst detection function since essentially all microbursts at this site are "wet" and therefore exhibit high radar reflectivity. Detection of the much less reflective thin-line signatures associated with gust fronts is substantially degraded, with the net lowering of system sensitivity. For these reasons we have not attempted to quantify WSP gust front detection capability at the Huntsville site. The later Orlando data sets, collected with a more appropriate set of radar and receive chain parameters, provide gust front detection results representative of what would likely be achieved at Huntsville with the WSP.

##### B. Truth Sensors

Figure 4 shows the location of relevant sensors during the Huntsville field measurements. An essentially co-located C-band 1.4° pencil-beam weather radar (operated under subcontract to the MIT Center for Meteorology) provided the primary source of truth for evaluation of the WSP algorithms. This is a coherent-on-receive magnetron system, providing good sensitivity—we estimate that the radar can measure reflectivity and Doppler velocity to 30 km for weather exceeding 0 dBz reflectivity.

##### C. Environmental Characteristics

Huntsville typically has 57 thunderstorm days per year with about one-half of these occurring during the summer months (June-August). The combination of significant low-level moisture and strong daytime surface heating in the absence of significant vertical wind shear leads to the occurrence of "air-mass" thunderstorms during the summer months. From fall to early spring, however, thunderstorms here are induced by strong frontal systems associated with considerable vertical shear due to the proximity of the polar jet stream. Microbursts in Huntsville are "wet," i.e., characterized by core radar reflectivities greater than 30 dBZ and measurable surface precipitation.



AIRPORT SURVEILLANCE RADAR  
WEATHER RESEARCH FACILITIES  
HUNTSVILLE, AL  
1987-1988

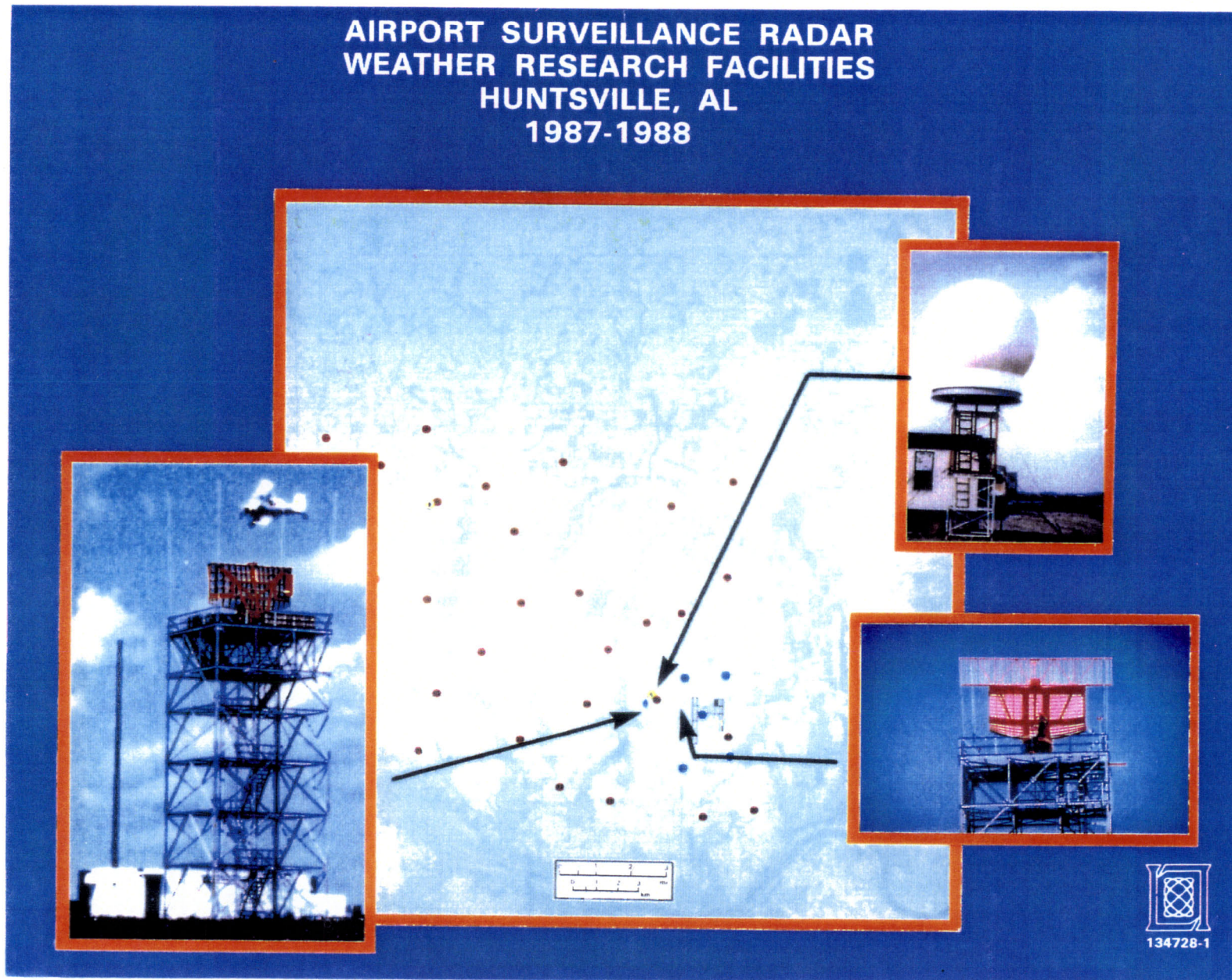


Figure 4. Map showing locations of FAA/Lincoln Laboratory ASR-8 testbed, supporting C-band pencil-beam "truth radar" and Mesonet anemometer during 1987-1988 Huntsville campaign.

The gust fronts observed by the TDWR testbed when located in Huntsville during the summer of 1987 were characterized by moderate reflectivity and moderate to strong maximum convergence strengths. All of the events in Huntsville had reflectivities between 10 and 30 dBZ. The majority of gust fronts were strong, with maximum convergence strengths between 15 and 25 m/s.

**D. Microburst Detection Performance**

Storm data from five different days in Huntsville were scored to characterize microburst detection algorithm performance in the Huntsville environment. This relatively small database (approximately 3-1/2 hours total, involving 30 separate microburst events) was chosen as representative of the storms that occurred near the prototype over the two-year operating period. Approximately 2500 images of WSP and “truth” radar imagery were compared for the evaluation. Difficulties in recovering Huntsville data, caused by aging digital tapes and subsequent changes in our prototype’s processing hardware/software, precluded scoring over the larger databases employed at subsequent operating sites.

Table 1 lists microburst detection ( $P_d$ ) and false alarm ( $P_{fa}$ ) probabilities for this data set. Given uncertainty in exactly measuring these parameters using finite wind shear databases, the statistics in Table 1 are consistent with those derived from the very similar Orlando environment where “wet” microbursts associated with air mass thunderstorms are predominant. For the overall population of divergent shears, the  $P_d$  was 84 percent, increasing to 95 percent for events exceeding the 15 m/s “microburst alert” threshold. False-alarm probability decreases from 20 percent for all “loss” alerts to 13 percent for “microburst” alerts.

Note that the majority of “misses” and “false alerts” tabulated for the weak shear strength category are the result of relatively small discrepancies between the loss intensities reported by the WSP and the pencil-beam radar employed as “truth.” For example, a WSP differential velocity report of 11 m/s in association with a “truth” radar reading of 9 m/s would be tabulated as a false alert and reversed readings would constitute a “miss.” Operationally, it is doubtful that this class of “erroneous” WSP report would be perceived as incorrect. For this data set as for those at subsequent prototype operating sites, the arbitrary 10 m/s alert/no-alert threshold somewhat distorts (in a pessimistic direction) the extent to which measured performance statistics for weak divergent shears reflect the “operational” reliability of the product.

**Table 1  
ASR-9 Microburst Detection Algorithm Scoring Results for Huntsville**

<b>Event Strength</b>	<b><math>P_d</math></b>	<b><math>P_{fa}</math></b>
≥10 m/s	0.84	0.20
≥15 m/s	0.95	0.13
≥20 m/s	1.00	0.11

## **3.2 Kansas City, Kansas, 1989**

### **A. Testbed Configuration**

The WSP testbed was re-located to a rural site overlooking the Missouri River valley some 15 km southwest of Kansas City International Airport (Figure 5). The site was characterized by relatively intense ground clutter from the bluffs of the Missouri River valley and the rolling terrain. As in Huntsville, the radar parameter settings significantly reduced sensitivity relative to later WSP designs, with the primary expected impact being on gust front detection. For this reason we again do not present a statistical analysis of the WSP's gust front detection capability in Kansas City.

### **B. Truth Sensors**

As shown in Figure 5, the WSP testbed was essentially co-located with the FAA/Lincoln Laboratory Terminal Doppler Weather Radar (TDWR) prototype, FL-2. At that time, this radar operated at S-band, producing a  $1^\circ$  pencil beam. Over the range of concern for evaluation of the WSP products (30 km), FL-2 had sensitivity sufficient to reliably measure reflectivity and Doppler velocity for wind shear phenomena with reflectivity of approximately -5 dBz or greater. The Klystron transmitter provided excellent stability, thereby supporting ground clutter suppression approaching -50 dB. In most cases, FL-2 performed a  $120^\circ$  sector scan centered on the airport. Full PPI scans at the surface were performed only once every five minutes. Unfortunately, the University of North Dakota pencil-beam radar that was also deployed to support the FAA wind shear measurements at Kansas City likewise performed a sector scan over the airport and did not provide significant coverage in this back sector. Thus, full scoring of the WSP testbed's products was limited to about one-third of the area that would be of operational concern for an on-airport WSP.

### **C. Environmental Characteristics**

Kansas City experiences an average of 50 thunderstorm days annually. Average yearly precipitation is approximately 35 inches, most of which falls between April and September. Measurable precipitation occurs on 105 days per year on average. Like Huntsville, average daily summer high temperatures are in the mid to upper 80's, and daily low temperatures fall to the 65-70 degree range during summer. Again, this suggests plentiful low-level moisture to fuel convective activity, but the prevalence of nocturnal low-level jet streams over the midwestern U.S. sustains thunderstorm development (non air-mass) into the nighttime hours. Data collected by the TDWR testbed indicates that about one-half of all Kansas City microbursts are hazardous to aviation (stronger than 15 m/s) and that they are predominantly wet. Median reflectivity factor (~45 dBz), however, is substantially less than was observed in either Huntsville or subsequently in Orlando (~50dBz).



Figure 5. Map showing locations of FAA/Lincoln Laboratory WSP and TDWR testbeds at Kansas City and supporting University of North Dakota radar.

A more significant difference relative to these southeastern U.S. sites is the presence of strong, vertical speed and direction shear in the ambient horizontal wind field in which Midwestern thunderstorms form. This shear serves to organize the convection into long-lived, meso-scale complexes that propagate rapidly and for long distances. Associated “sloping” of precipitation shafts is a significant issue for low-altitude wind shear detection with the ASR-9’s fan beams. In some circumstances, reflectivity aloft may exceed that at the surface by many orders of magnitude, making it virtually impossible for the radar to measure the near-surface wind field accurately. This circumstance does not directly affect the ability to detect microbursts since, as indicated above, these are predominantly associated with surface rain. However, false divergent velocity signatures may result when changes in wind with altitude are “interpreted” by the fan beam as horizontal wind shear.

#### D. Microburst Detection Performance

False divergence signatures generated by the sloping storm structures described above are most prevalent near the edges of storm cells, or in other regions where the vertically integrated reflectivity seen by the ASR’s beam has a significant horizontal gradient. To reduce the occurrence of false alarms from this mechanism, the verification stage of the WSP’s microburst detection algorithm aggressively filters out divergence signatures that are centered outside the significant reflectivity contours in a storm cell. Although this and other image processing techniques are effective in holding false alert probabilities down, in some cases they may also eliminate alerts for true divergent shears.

Detection and false-alarm statistics from the Kansas City database are listed in Table 2. Data are from a representative set of thunderstorm episodes, acquired on ten different days. The database encompasses six hours in total, and 45 discrete microbursts. Forty-three hundred images of WSP and “truth” radar were scored. These periods include most of the significant convection that occurred at the test site during the Kansas City campaign.

**Table 2**  
**ASR-9 Microburst Detection Algorithm Scoring Results for Kansas City**

Event Strength	$P_d$	$P_{fa}$
$\geq 10$ m/s	0.67	0.21
$\geq 15$ m/s	0.87	0.15
$\geq 20$ m/s	0.99	0.09

Relative to southeastern U.S. airmass thunderstorm environments, the  $P_d$  at Kansas City was lower, particularly for divergent wind shears below the “microburst alert” threshold. Overall, about two-thirds of all divergent shears were detected by the prototype, rising to almost 90 percent at the 15 m/s “microburst threshold. Higher detection probabilities in this environment could readily be attained if  $P_{fa}$  were allowed to rise.

### **3.3 Orlando Florida, 1990-1992**

#### **A. Testbed Configuration**

The WSP testbed was moved to Orlando, Florida in the spring of 1990, along with the TDWR prototype and other supporting sensors. The WSP testbed occupied the former on-airport site of the FAA's operational radar (ASR-8) which had been vacated upon commissioning of its ASR-9. During the Orlando field program, the host radar for the WSP prototype was upgraded from an ASR-8 to an ASR-9, and the WSP receiver's dynamic range was increased substantially. Gust front detection was identified as a system requirement so that, in contrast to previous operations, a database was acquired that was appropriate for quantitative evaluation of WSP gust front capability.

#### **B. Truth Sensors**

Figure 6 shows the locations of supporting sensors deployed during operations in Orlando. As in Kansas City, the FL-2 TDWR prototype was generally the preferred reference for scoring of WSP products. For operations in Florida, this radar was converted to the C-band operating frequency used in the production TDWR. Because FL-2 was not co-located with the WSP testbed, radar viewing angles for some wind shear events differed significantly between the two radars. When there was concern that asymmetry in the strength of microburst outflow winds might be a factor in differences between WSP and TDWR testbed measurements of a microburst, we examined data from either the University of North Dakota or MIT C-band weather radars (whichever had a viewing angle to the event most similar to the WSP testbed) to arbitrate.

#### **C. Environmental Characteristics**

Orlando averages about 80 thunderstorm days per year. More than fifty of these occur during the summer months. Precipitation is measurable on 116 days per year on average, and the mean annual total is approximately 50 inches, most of that received in the summer. Average daily high temperatures during summer months are in the low 90's, while daily lows range from 70 to 75 degrees, corresponding to the highest summertime dewpoints in the continental U.S. Thus, air-mass thunderstorms form almost daily at this time of year, often aided by the propagation of sea-breeze fronts that migrate eastward and/or westward over the Florida peninsula. Since these phenomena are instigated by daytime surface heating, most summertime microbursts in Florida occur during the daylight hours, with a few lingering into the early evening. As mentioned previously, all microbursts in the southeastern U.S. are classified wet. Median core reflectivities in Orlando microbursts were measured to be 50dBz.

Gust fronts observed in Orlando were characterized by low to moderate thin line reflectivity values and weak convergence strengths. Median gust front thin line reflectivity was 15 dBz. Seventy-two percent of Orlando gust fronts exhibited maximum convergence strength less than 10 m/s.

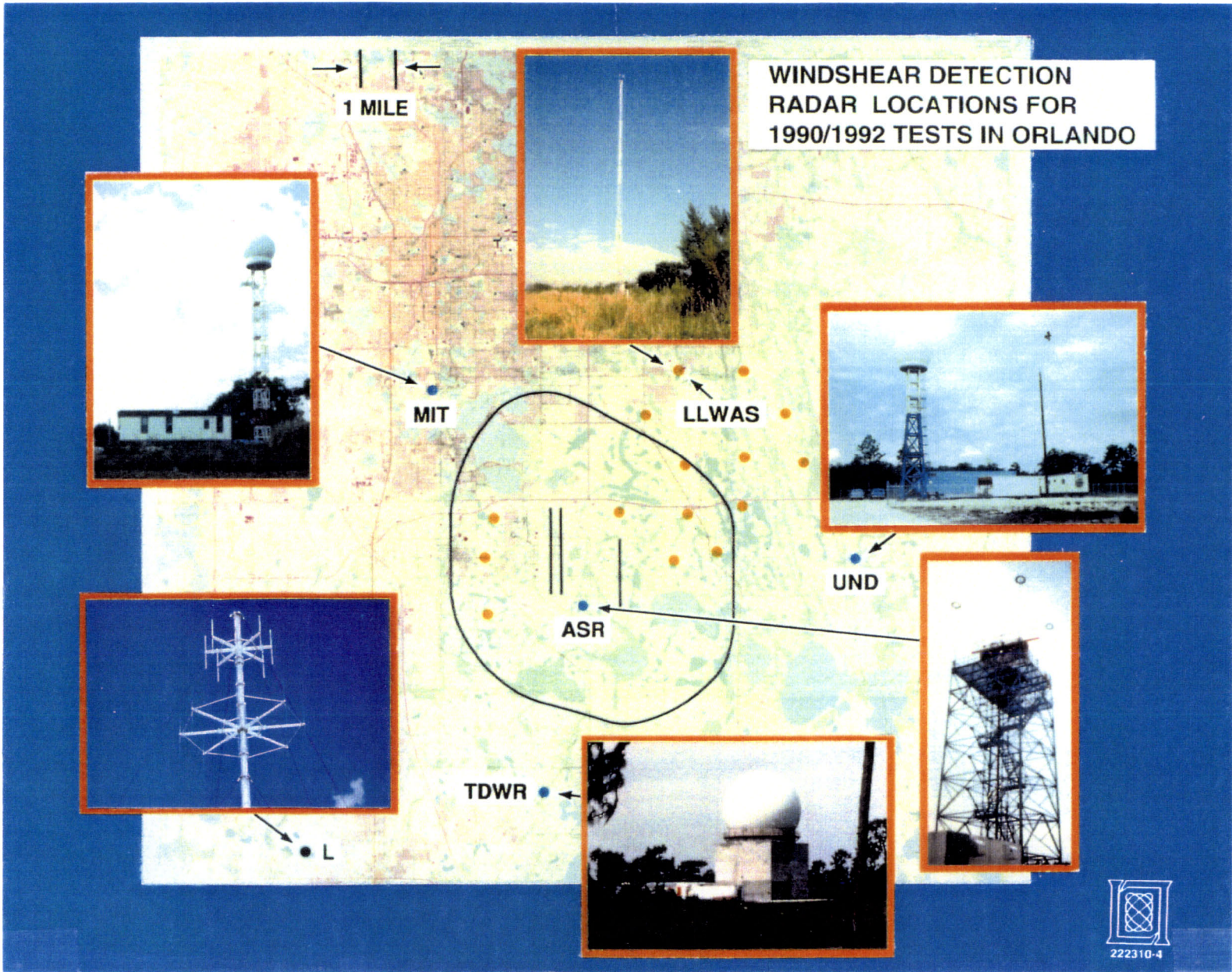


Figure 6. Map showing locations of sensor deployed in Orlando, Florida during TDWR and WSP field measurement programs there.

#### D. Microburst Detection Performance

Table 3 lists detection and false-alarm statistics for the WSP's microburst detection function operated over the three years of the Orlando field program. The database is from thunderstorm episodes on 34 days during this period, encompassing approximately 30 hours of convective storm activity and 200 discrete microburst events. Twenty-one thousand single-scan images from the WSP and truth radars were scored.

As in Huntsville, the prevalence of air mass (weakly sheared) thunderstorm cells, high radar cross sections in microbursts and the benign clutter environment contribute to a high overall probability of detection and low to moderate false-alarm probabilities for all strength categories. The  $P_d$  at the microburst alert threshold is 91 percent, with an associated false-alarm probability of six percent.

**Table 3**  
**ASR-9 Microburst Detection Algorithm**  
**Scoring Results for Orlando**

Event Strength	$P_d$	$P_{fa}$
$\geq 10$ m/s	0.80	0.12
$\geq 15$ m/s	0.91	0.06
$\geq 20$ m/s	0.96	0.04

#### E. Gust Front Detection Performance

Data from eight thunderstorm days during the 1991 and 1992 storm seasons were evaluated to estimate WSP gust front detection performance in the Orlando environment. Approximately 630 images of WSP and TDWR data were compared, encompassing more than 25 hours of data collection. Statistics summarizing detection performance are presented in Table 4. The detection probability for fronts with associated convergent velocity differential exceeding 10 m/s was 67 percent, increasing to 73 percent for fronts with  $\Delta V \geq 15$  m/s.

**Table 4**  
**ASR-9 Gust Front Detection Algorithm**  
**Scoring Results for Orlando**

	$\Delta V \geq 10$ m/s	$\Delta V \geq 15$ m/s	$P_{fa}$
$P_d$	0.67	0.73	0.11



### **3.4 Albuquerque, New Mexico, 1993-1995**

#### **A. Testbed Configuration**

The testbed was relocated to Albuquerque International Airport (ABQ) in the spring of 1993 for data collection and operational demonstrations in an arid, High Plains environment. An on-airport site with unobstructed viewing to the runways and principal approach and departure corridors was chosen. Our testbed siting choices differ significantly from those the FAA employed in siting its ASR-9 at Albuquerque. The FAA's radar is sited in a natural depression (serving as a clutter fence for the radar), and its antenna is tilted upwards  $0.5^\circ$  relative to the normal ASR setting. These choices reduce interference from the severe ground clutter at ABQ but also reduce radar illumination at low altitude where wind shear phenomena are most manifest. It is unclear whether the differences in our siting and antenna tilt, relative to those used for the FAA's radar at Albuquerque, would lead to a net increase or decrease in wind shear detection performance.

#### **B. Truth Sensors**

The MIT C-band radar used previously in Orlando and Huntsville was deployed at a site approximately 3 nmi south of the WSP testbed as our primary source of truth for the WSP's wind shear products (Figure 7). As noted previously, this radar's sensitivity is adequate to detect wind shear with reflectivity of 0 dBz or greater. However, limited clutter suppression capability associated with the radar's magnetron transmitter makes accurate measurement of low reflectivity weather echoes problematic in intense ground clutter areas around ABQ. In most cases, the spatial extent of the wind shear phenomena is sufficiently large relative to the clutter-obscured area that a human data interpreter can adequately truth the event. In the circumstance where actual wind shear events were invisible to our truth radar—an event we believe was rare, based on visual observations of wind shear cues and wind data from the MESONET array shown in Figure 7—the effect would have been to undercount the occurrence of missed detections (if the WSP likewise did not detect the event) or over count false alarms (if the WSP did detect the event).

#### **C. Environmental Characteristics**

Albuquerque International Airport is located on a plateau south of the city of Albuquerque. The terrain rises steadily to the east and northeast before reaching the shear faces of the Sandia Mountains. These extend at their highest elevation more than 1800 m above the altitude of the airport. To the west, the terrain falls off 100 meters or more to the Rio Grande River Valley, then rises steadily over many miles to a level approximately 120 m higher than that of the airport. Ground clutter resulting from this significant topographic relief is extreme. In addition to the topography, large hangars and buildings on Kirtland Air Force Base to the northeast of the testbed produce extremely intense discrete clutter sources at short range. The median equivalent weather reflectivity factor for clutter within 15 km of the testbed is 32 dBz, and in 10 percent of the resolution cells within this range, equivalent clutter reflectivity exceeds 60 dBz.

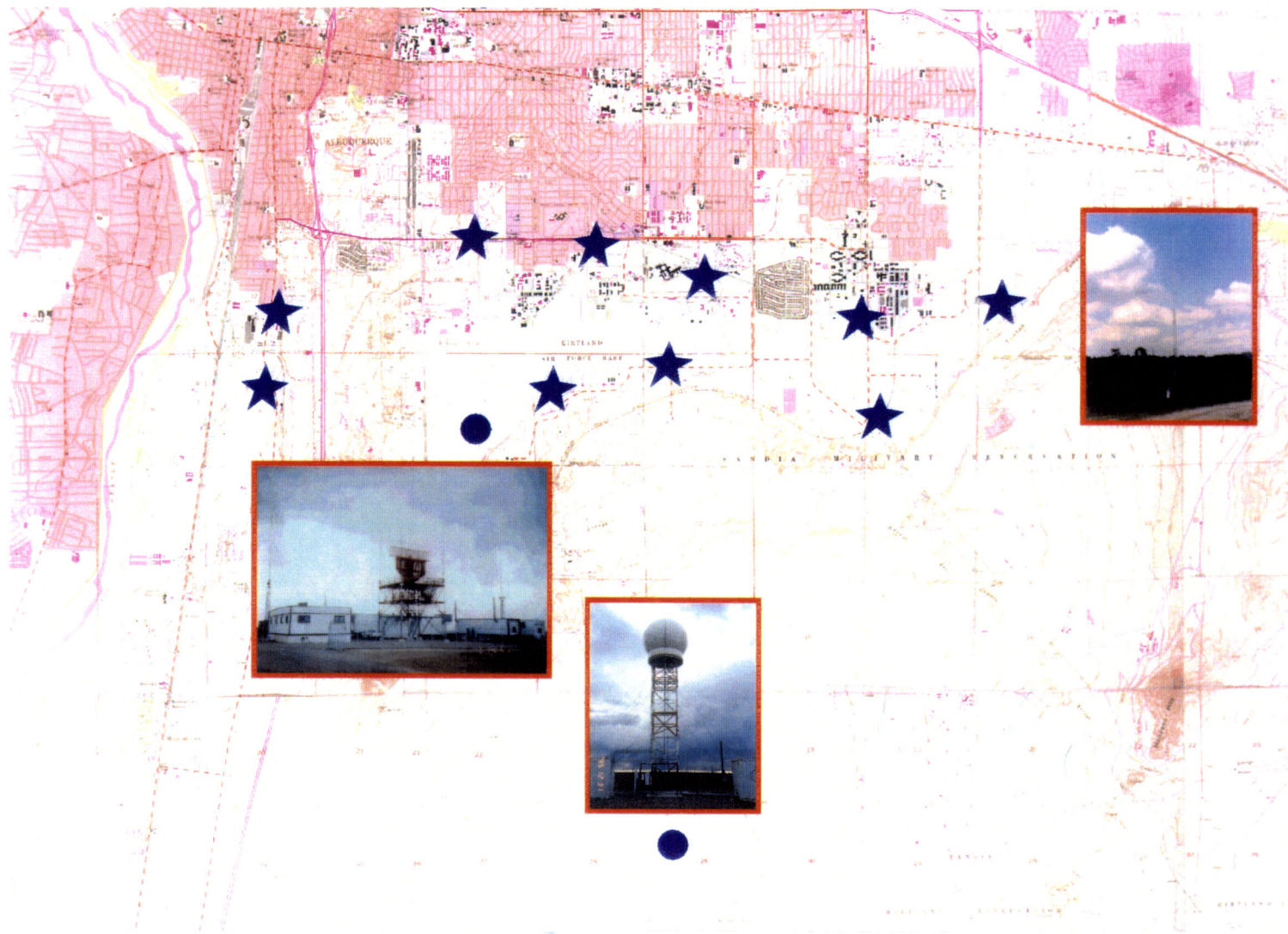


Figure 7. Map showing locations of WSP testbed, MIT "truth" radar, and anemometers at Albuquerque.

On average, 42 thunderstorm days per year occur in Albuquerque. More than one-half of these occur in late summer (July-August) in conjunction with the monsoon season in the desert Southwest. Measurable precipitation is received on only 61 days per year on average, and the mean annual total precipitation is only about 8.5 inches, most of which falls during the monsoon. Average daily high temperatures in summer are consistently around 90°, with average daily low temperatures falling to the upper 50's and low 60's. Summertime thunderstorms are air-mass type, but peak occurrence is in early evening, possibly delayed by a "deficit" of atmospheric moisture, relative to other testbed locations.

This relative lack of moisture is also evident in the frequent occurrence of *dry* microbursts in Albuquerque which have relatively low radar reflectivities and little or no surface rainfall. Approximately 25 percent of Albuquerque microbursts exhibit core reflectivities of less than 30 dBz. Such events exhibit radar cross sections that may be many orders of magnitude smaller than the severe ground clutter sources that are prevalent at this site. Compounding the difficulty of radar-based microburst detection at this site is the presence of significant vertical shear in the ambient wind field caused by topographic effects and the frequent proximity of synoptic fronts. We described the effects of vertical shear on WSP microburst detection capability in discussing the Kansas City results.

The arid ABQ environment is also manifest in the radar reflectivities of gust front thin lines. Essentially all of the gust fronts observed had reflectivities less than 10 dBZ, and 35 percent had reflectivities less than 0 dBz. The speed of movement and convergence strength associated with many of these fronts were strong, however. In particular, "Canyon Wind" events—outflows from thunderstorms east of the Sandia Mountains, which are funneled through the Tijeras canyon onto the airport—are normally very strong, with maximum convergence strengths greater than 15 m/s. Radar detection of these events is extremely difficult until they clear the intense ground clutter from the mountains.

#### **D. Microburst Detection Performance**

Table 5 summarizes detection and false-alarm probabilities for the WSP prototype's microburst detection function at ABQ. Data evaluated were from 38 representative thunderstorm days during the 1993 and 1994 storm seasons. Approximately 35 hours of data are included, involving 120 separate microburst events. Twenty-five thousand scans of WSP and truth radar data were scored in generating these statistics.

The environmental challenges of this site—severe ground clutter, low cross section microbursts and a high-wind, vertically sheared ambient atmosphere—resulted in significant reduction in  $P_d$  relative to the other sites evaluated. Two-thirds of all divergent wind shears were detected by the WSP prototype, rising to approximately 80 percent at the microburst alert threshold. Higher false-alarm probabilities also were incurred, particularly for weak shear alerts near the 10 m/s threshold.

**Table 5**  
**ASR-9 Microburst Detection Algorithm**  
**Scoring Results for Albuquerque**

Event Strength	$P_d$	$P_{fa}$
$\geq 10$ m/s	0.66	0.29
$\geq 15$ m/s	0.78	0.18
$\geq 20$ m/s	0.92	0.13

**E. Gust Front Detection Performance**

Gust front detection results from Albuquerque are summarized in Table 6. This data set was drawn from six representative days in 1994. (The WSP receive chain configuration was improved following the 1993 ABQ storm season to realize increased sensitivity for the very low radar cross section gust fronts prevalent at this site, resulting in a substantial improvement in gust front detection performance.) Fifteen hours of data, encompassing 422 comparisons of WSP and truth radar imagery, are included in the database.

As with the microburst detection algorithm, the sensitivity constraints of the ASR-WSP and the presence of strong clutter regions inhibited the gust front algorithm's detection ability. Due to the low reflectivity associated with many of the gust fronts, the events were often barely visible in the base data, especially those located near clutter regions. In spite of these challenges, the algorithm did very well with the stronger gust fronts, detecting 74 percent of the gust fronts having  $\Delta V > 15$  m/s. Weaker gust fronts were more difficult to observe by the WSP. The  $P_d$  for all fronts with  $\Delta V$  exceeding 10 m/s was 50 percent.

**Table 6**  
**ASR-9 Gust Front Detection Algorithm**  
**Scoring Results for Albuquerque**

	$\Delta V \geq 10$ m/s	$\Delta V \geq 15$ m/s	$P_{fa}$
$P_d$	0.50	0.74	0.11

#### 4.0 INTERPRETATION OF RESULTS RELATIVE TO WSP NATIONAL DEPLOYMENT PLANS

Estimates of WSP wind shear detection performance at all sites scheduled to receive the WSP can be achieved via a climatology-based extrapolation of the testbed scoring results reported here. Analysis of climatological data for the proposed WSP locations permits separation of the sites into groups of homogeneous climatology that can be used to project ASR-WSP wind shear detection performance at locations for which we have not collected testbed data. The climatological data used for this analysis include 30-year normals for annual number of thunderstorm days, measurable-precipitation days and the average hour of maximum thunderstorm occurrence. These parameters for the 33 ASR-WSP airports are listed in Appendix A. In Table 7 we project detection performance for the major safety hazard addressed by the WSP, divergent shears with differential velocity exceeding 15 m/s (microburst alerts).

Thunderstorms in the northeast U.S. occur mainly during the summer months in late afternoon and are often triggered by fronts associated with low-pressure systems traversing southern Canada. In these situations, significant vertical shear in the ambient wind is likely to be present, possibly leading to contamination of the ASR-WSP surface velocity estimates from above-ground storm features as in Kansas City. In other instances, conditions favor air-mass-thunderstorm development typical of the southeastern U.S. Given this knowledge, we would expect wind shear detection performance to fall between the Kansas City and southeastern U.S. testbed results. Ten WSP sites fall into this environmental regime.

Another distinct climatological region exists in the upper-midwestern U.S. and includes the ASR-WSP sites of Madison, Cedar Rapids and Des Moines. These locations exhibit slightly more thunderstorm days than those in the northeastern U.S. and a nocturnal peak in thunderstorm frequency. The nocturnal peak is attributable to this region's closer proximity to the main jet stream and nocturnal low-level jets during the summer months. The strong dynamics associated with these features sustain thunderstorm development beyond the hours of daytime surface heating. Consequently, vertical wind shear is likely to be significant in this regime during thunderstorm periods as was observed when the ASR-WSP testbed collected data in Kansas City in 1989. Therefore, we would expect microburst detection performance at these three WSP locations to mirror the Kansas City testbed results cited earlier.

The southeastern U.S. comprises a third climate zone. The 11 ASR-WSP sites in the Southeast have approximately the same number of days with measurable precipitation, but the hour of maximum thunderstorm frequency is slightly earlier on the Southeast coast and Florida peninsula, primarily due to sea-breeze enhancement. Cities here also have more thunderstorm days, while those farther north experience significant snowfall on at least one day annually. However, the predominant type of thunderstorm throughout the Southeast is the air-mass thunderstorm driven by diurnal surface heating during the summer months and promoted by sea-breeze fronts if near the Southeast coast. Hardly any vertical shear in the ambient wind is present in both regimes during the summer, so interference with ASR-WSP surface-velocity estimating capability is minimal. We would expect wind shear detection performance statistics at the 11 WSP Southeast sites to be well represented by data gathered at the Huntsville and Orlando WSP testbed sites.

The ASR-WSP sites in southern Texas are distinct from other Southwestern sites in their early hour of maximum thunderstorm frequency (high convective available potential energy) and absence of vertical wind shear most of the year. Summertime thunderstorms are usually air-mass type, with Gulf of Mexico moisture fueling the activity. Therefore, we would expect wind shear detection performance for the three south Texas sites to reflect Orlando/Huntsville performance.

The second climatological group of Southwest sites (Lubbock, El Paso, Tuscon and Albuquerque) will experience atmospheric moisture conditions representative of Albuquerque, although vertical wind shear and ground clutter may be significantly lower than ABQ. As mentioned previously, the operational issue unique to this region is the occurrence of dry microbursts, mainly in late spring/early summer, which ASR-WSP may not detect if the events are very dry. Most thunderstorm activity occurs during the later summer months when moist monsoonal flow enters the region. Vertical shear in the ambient wind has been evident in Albuquerque during the summer months, although this may be less of an issue at more southerly sites owing to greater distance from polar fronts. Expected WSP performance at these sites would be similar to Albuquerque although Southwest sites with less ground clutter might show improved results.

Finally, thunderstorm frequency in southern California and Hawaii is lowest of all the ASR-WSP sites. Cold fronts associated with coastal-Pacific winter storms are often the cause of those in the Los Angeles area. We would suspect sea breezes and terrain induce most thunderstorms in Hawaii. Vertical wind shear should not pose a problem for surface velocity estimation at either location, except during the winter months in Los Angeles when the polar jet stream occasionally dips southward toward the area. Our best estimate is that detection performance in southern California would be in the range of that demonstrated at the prototype's southeastern and midwestern U.S. sites, and that Hawaii's would closely resemble Orlando's since both locations are tropical.

**Table 7**  
**Projected WSP Microburst Detection Performance**  
**Within Climatological Regimes ( $\Delta V \geq 15$  m/s )**

<b>Climate Region</b>	<b>Number Of Sites</b>	<b>Expected <math>P_d</math></b>	<b>Expected <math>P_{fa}</math></b>
Northeast	10	0.85 - 0.90	0.10 - 0.15
Midwest	3	0.85 - 0.90	0.15 - 0.20
Southeast/Florida	11	0.90 - 0.95	0.05 - 0.15
SouthCentral	3	0.90 - 0.95	0.05 - 0.15
Southwest	4	0.75 - 0.85	0.15 - 0.20
Southern California	2	0.85 - 0.95	0.10 - 0.15
Hawaii	1	0.90 - 0.95	0.05 - 0.15

## 5.0 PERFORMANCE OF CURRENT GROUND-BASED WIND SHEAR DETECTION SYSTEMS

For comparison with the WSP performance metrics given in the preceding chapters, we briefly summarize corresponding data on current FAA ground-based wind shear detection equipment. Findings are summarized in Table 8. Note that, where quoted, microburst  $P_{fa}$  estimates apply to all divergent loss alerts.

The six-station Low Level Wind Shear Alert System (LLWAS) is the current wind shear detection system at all airports slated to receive the WSP enhancement to their ASR-9. LLWAS operates by comparing measurements of wind speed and direction at an airport centerfield anemometer with five surrounding anemometers. "Airport quadrant" wind shear alerts are generated when significant wind differences are identified among the sensors. LLWAS does not explicitly indicate the loss or gain associated with a wind shear nor does it localize its position beyond identifying the affected quadrant. The LLWAS anemometer network coverage does not typically extend significantly beyond the runway thresholds.

LLWAS was originally designed for gust front phenomena and as such exhibits high (greater than 0.9) probability of alert when gust fronts reach the sensor network [W. Wilson, personal communication]. Over the area of coverage specified for the ASR-WSP—coverage to three miles out from runway thresholds on the arrival corridor and two miles out on departures—this translates to an equivalent  $P_d$  of roughly 0.4. Here we assume that the LLWAS network covers nominally 2 mi runway lengths and 1/2 mi beyond the runway thresholds. The in-network detection probability is scaled according to the proportion of operationally significant airspace not covered by the anemometer network:

$$\begin{aligned} \text{Scaling Factor} &= \frac{[2\text{mi}(\text{rwy}) + 0.5\text{mi}(\text{arr}) + 0.5\text{mi}(\text{dep})]}{[2\text{mi}(\text{rwy}) + 3\text{mi}(\text{arr}) + 2\text{mi}(\text{dep})]} \\ &= \frac{3}{7} = 0.43 \end{aligned}$$

LLWAS network design is considerably less favorable for detection of small-scale microburst wind shear. Estimated  $P_d$  within the sensor network is roughly 0.6 [Wilson and Cole, 1993]. When scaled to the areal coverage specified for the WSP, this is reduced to an effective  $P_d$  of 0.3. When LLWAS sensors are well sited and free of sheltering effects, the false-alarm probability is low. Unfortunately, many current LLWAS networks have some sheltered anemometers; during strong environmental flow conditions, these result in persistent false alarms due to apparent shear between sensors that respond to the environmental winds and those that do not. We have not attempted to estimate the average LLWAS false-alarm probability.

Network Expansion LLWAS (NE-LLWAS) addresses the above deficiencies by increasing the density of anemometers and extending network coverage as required on approach and departure corridors. Anywhere from 12 to more than 20 anemometers may be required for appropriate coverage at a given airport. NE-LLWAS provides runway-specific alphanumeric alerts in a format identical to that provided by the Terminal Doppler Weather Radar (TDWR) and the WSP. NE-LLWAS is highly effective for wind shear detection: stated detection

probabilities for microburst strength losses are in excess of 0.95, with a corresponding PFA of less than 0.05 [ Wilson and Gramzow, 1991; Wilson and Cole, 1993]. Unfortunately, widespread implementation of NE-LLWAS has been prohibited by the system's high costs for deployment and life-cycle maintenance. In addition, FAA Air Traffic and Airway Facilities sponsors have preferred radar-based wind shear detection systems because:

1. The broad-area weather surveillance (e.g., storm location and movement, gust front movement) provided by the radar systems enhances Air Traffic situational awareness and thereby facilitates traffic management during adverse weather.
2. Real-estate procurement, installation and maintenance efforts are high for the multi-station NE-LLWAS system.

Terminal Doppler Weather Radars (TDWR) have been procured for 45 large airports in the continental U.S. The system is built around a dedicated, high-resolution Doppler weather radar capable of precision measurement of low-altitude wind shear phenomena. The  $P_d$  for microburst strength wind shear measured with the FAA/Lincoln Laboratory prototype TDWR equalled or exceeded 0.95 at all sites, with associated low false-alarm probabilities [Evans, 1990; Bernella, 1991; Campbell, 1989]. TDWR gust front detection capability is somewhat lower. (Note that in the Kansas City prototype TDWR results cited in Table 8, radar viewing angle at the airport was poor from a gust front detection viewpoint.) TDWR deployment has been limited to 45 airports owing to the high procurement, deployment and life-cycle maintenance costs of the dedicated weather radar system.

**Table 8**  
**Performance Summaries for Current Ground Based**  
**Wind Shear Detection Equipment**

System	Microburst > 15 m/s	Gust Front > 10 m/s	Climatic Regions Applicable
LLWAS	$P_d$ : 0.3 $P_{fa}$ : ?	$P_d$ : 0.4 $P_{fa}$ : ?	All
NE- LLWAS	$P_d$ : 0.97 $P_{fa}$ : 0.03	$P_d$ > 0.95 $P_{fa}$ > 0.05	All
TDWR	$P_d$ : 0.95 $P_{fa}$ : 0.04	$P_d$ : 0.79 (0.55) * $P_{fa}$ : 0.06 (0.00)	Southeast U.S. (Orlando)
	$P_d$ : 0.99 $P_{fa}$ : 0.11	$P_d$ : 0.77 (0.45) $P_{fa}$ : 0.13 (0.40)	Midwest U.S. (Kansas City)
	$P_d$ : 0.95 $P_{fa}$ : 0.06	$P_d$ : 0.78 (0.70) $P_{fa}$ : 0.02 (0.00)	Southwest U.S. (Denver)
* Parenthetical $P_d$ s and $P_{fa}$ s reflect scoring of gust fronts impacting airport. Other numbers apply to all gust fronts within range of radar.			



## 6.0 SUMMARY

In this report, we have provided background and a quantitative performance summary for the wind shear detection functions (microburst and gust front) of the Airport Surveillance Radar Weather Systems Processor. The current prototype WSP hardware and algorithms are viewed as largely representative of what will be deployed in the production version of the WSP, although some improvements in performance may accrue from refinement efforts that will be ongoing up to the time of full-scale development (FSD) contract award. The algorithms will be provided at that time by the Government to the FSD contractor for implementation.

Overall, we believe that the analysis in this report supports the contention that the WSP's wind shear detection algorithms—at their current level of performance—will provide operational products sufficient to meet the needs of the aviation community at the airports where the system will be deployed. Challenging environmental conditions—such as those experienced during testbed operations at Kansas City and Albuquerque—may degrade performance relative to the near-TDWR-like capability demonstrated in the southeastern U.S. Operational feedback, however, during our recent Albuquerque demonstrations indicate—as was the case during the earlier Orlando, FL demonstrations—that the wind shear detection performance of the prototype WSP is viewed extremely positively by Air Traffic Controllers and pilots. Informal feedback and questionnaires filled out by users at both airports have documented that the WSP's wind shear products, in combination with its predictions of flight route impact through gust front tracking and storm motion estimation, have significantly improved the safety and efficiency of terminal operations.

**APPENDIX A  
CLIMATOLOGICAL DATA FOR PROPOSED WSP SITES**

<b>LOCATION / FAA REGION</b>	<b>ANNUAL # OF T-STORM DAYS</b>	<b>HOUR OF MAX FREQUENCY (LT)</b>	<b>ANNUAL # OF DAYS WITH: PRECIP &gt;0.01"</b>	<b>SNOWFALL &gt;1.0"</b>
Providence, RI / New England	20	1700	124	10
Hartford, CT / New England	21	1700	127	13
Albany, NY / Eastern	26	1700	134	16
Islip, NY / New England	25	1800	116	8
Harrisburg, PA / Eastern	32	1800	124	9
Fort Wayne, IN / Great Lakes	39	1700	131	10
Syracuse, NY / Eastern	28	1700	170	33
Rochester, NY / Eastern	29	1700	158	27
Buffalo, NY / Eastern	31	1800	168	27
Grand Rapids, MI / Great Lakes	35	1800	144	2
Madison, WI / Great Lakes	40	0200	119	13
Cedar Rapids, IA++ / Central	41	0200	101	10
Des Moines, IA / Central	49	0200	107	10
Richmond, VA / Eastern	37	1800	113	4
Norfolk, VA / Eastern	36	1700	115	2
Greensboro, NC / Southern	45	1800	116	3
Knoxville, TN / Southern	47	1500	126	4
Huntsville, AL / Southern	57	1600	116	1
Birmingham, AL / Southern	58	1700	116	1
Charleston, SC / Southern	56	1600	112	0
Jacksonville, FL / Southern	65	1500	115	0
Gainesville, FL / Southern	79	1600	116	0
Daytona Beach, FL / Southern	77	1500	114	0
Sarasota, FL* / Southern	86	1600	107	0

**APPENDIX A  
(Continued)**

LOCATION / FAA REGION	ANNUAL # OF T-STORM DAYS	HOUR OF MAX FREQUENCY (LT)	ANNUAL # OF DAYS WITH:	
			PRECIP >0.01"	SNOWFALL >1.0"
Austin, TX / Southwest	41	1400	83	0
San Antonio, TX / Southwest	37	1400	81	0
Harlingen, TX** / Southwest	26	1300	73	0
Lubbock, TX / Southwest	47	2000	63	3
El Paso, TX / Southwest	36	1800	48	2
Albuquerque, NM / Southwest	42	2000	61	2
Tuscon, AZ / Western Pacific	42	2000	53	1
Los Angeles, CA / Western Pacific	4	N/A	36	0
Ontario, CA+ / Western Pacific	4	N/A	36	0
Honolulu, HI / Western Pacific	7	N/A	100	0
Climatological data for: *Tampa, FL ** Brownsville, TX + Los Angeles, CA ++ Waterloo, IA				

## REFERENCES

Weber, M.E., "Ground Clutter Processing for Wind Measurements with Airport Surveillance Radars," Lexington, Massachusetts, M.I.T. Lincoln Laboratory, DOT/FAA/PM-87/21, Project Report ATC-143, 4 November 1987.

Weber, M.E., "Dual-Beam Autocorrelation Based Wind Estimates from Airport Surveillance Radar Signals," Lexington, Massachusetts, M.I.T. Lincoln Laboratory, DOT/FAA/PS-89/5, Project Report ATC-167, 21 June 1989.

Newell, O.J. and J.A. Cullen, "ASR-9 Microburst Detection Algorithm," Lexington, Massachusetts, M.I.T. Lincoln Laboratory, DOT/FAA/NR-93/2, Project Report ATC-197, 22 October 1993.

Delanoy, R.L., and S.W. Troxel, "Machine Intelligent Gust Front Algorithm," Lexington, Massachusetts, M.I.T. Lincoln Laboratory, DOT/FAA/RD-93/1, Project Report ATC-196, 4 November 1993.

Weber, M.E., "Airport Surveillance Radar (ASR-9) Wind Shear Processor: 1991 Test at Orlando, FL," Lexington, Massachusetts, M.I.T. Lincoln Laboratory, DOT/FAA/NR-92/7, Project Report ATC-189, 1 June 1992.

Wilson, F.W. and R.H. Gramzow, "The Redesigned Low Level Wind Shear Alert System," Preprints: Fourth International Conference on Aviation Weather Systems, June 24-28, 1991, Paris, France, pp 370, AMS, Boston, MA.

Evans, J.E., "Results of the Kansas City 1989 Terminal Doppler Weather Radar (TDWR) Operational Evaluation Testing", Lexington, Massachusetts, MIT Lincoln Laboratory, DOT/FAA/NR-90-1, Project Report ATC-171, 17 August 1990.

Bernella, D.M., "Terminal Doppler Weather Radar Operational Test and Evaluation, Orlando 1990", Lexington, Massachusetts, MIT Lincoln Laboratory, DOT/FAA/NR-91-2, ATC-179, 9 April 1991.

Campbell, S.D., "Use of Features Aloft in the TDWR Microburst Recognition Algorithm", Preprints: Twenty-Fourth Conference on Radar Meteorology, March 27-31, 1989, Tallahassee, Florida, pp. 167, AMS, Boston, MA.

Wilson, F.W. and R.E. Cole, "LLWAS II and LLWAS III Performance Evaluation," Preprints: Fifth International Conference on Aviation Weather Systems, August 2-6, 1993, Vienna, VA, AMS, Boston, MA..

Wilson, F.W., personal communication, April 1996.